



Study on Corrosion Inhibition of Mild Steel in Aqueous Chloride Environment Using PABA as Green Inhibitor

**Albin Aloysius^{1*}, Rajajeyaganthan Ramanathan², Auxilia christy¹,
Noreen Anthony^{3*}**

¹Department of Chemistry, BWDA College, Kolliyanguam – 604304, Tamilnadu, India

²Department of Chemistry, M.Kumarasamy College of Engineering, Karur – 639113,
Tamilnadu, India

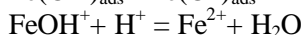
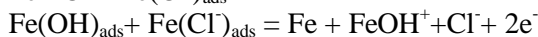
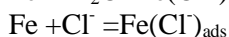
³Department of Chemistry, Holy Cross College, Tiruchirappalli – 620002,
Tamilnadu, India

Abstract : Corrosion inhibition studies of mild steel in 240 ppm aqueous chloride ion solution with p-amino benzoic acid (PABA) has been investigated using experimental techniques such as weight loss, Ultraviolet-Visible spectroscopy (UV), Fourier transform infrared spectroscopy (FTIR), Potentiodynamic Polarization (PDP), Electrochemical Impedance Spectroscopy (EIS) and Scanning Electron Microscopy (SEM). All these techniques revealed that the inhibitor PABA reduced the mild steel corrosion through their effective adsorption to form an inhibitive layer by Fe-inhibitor complex formation which is further evidenced from FTIR.

Keywords : Green corrosion inhibitor, Vitamin B10, p-Amino benzoic acid, Mild Steel, 240 ppm chloride medium.

1. Introduction

Corrosion of iron due to its contact with worst environments offers a serious economic problem. It was reported [1-3] that the corrosion of iron in corrosive solutions arises through the dissolution of iron from the oxidation state 0 to +2 and further to +3. When the solutions containing more concentration of chloride ions, the dissolution of iron from the oxidation state 0 to +2 arises on multistep as follows:



The corrosion and its inhibition of iron in various environments were reported in several research studies [4-8]. Among this, one of the important techniques to protect iron against corrosion is the usage of corrosion inhibitors [9-10]. The usage of green corrosion inhibitors have been widely reported by many authors [9-11]. The efficiency of these compounds is due to the presence of functional groups, steric effects, electronic density of donor atoms, and p-orbital character of donating electrons [9-15]. The inhibition mechanism is usually based on their interactions with the metal surface and their adsorption sites where polar functional groups are present [16]. The inhibitor molecules bonded to the metal surface may be due to chemisorption, physisorption, or complexation with the polar groups acting as the reactive centre in the molecules [17]. This study reports the inhibition of the electrochemical corrosion of iron in 240 ppm chloride ion solutions by

PABA with different electrochemical measurements. The structure of the compound is shown in Figure 1. The PABA contains two donor oxygen atoms and one amino group in their structure. These groups of PABA may act as reactive centre for inhibiting corrosion of mild steel.



Figure 1. Molecular and optimized Structure of PABA

2. Materials and Methods

The material used in this study was mild steel coupons with chemical composition (% wt.) of 0.10 C, 0.06 P, 0.40 Mn, 0.026 S and the remaining Fe. Mild steel coupons of dimension 1 x 4 x 0.2 cm³ were cut and scraped using 150–600 grit emery papers. The coupons were degreased and rinsed with AR grade acetone and double distilled water, respectively. FeSO₄ and NaCl were purchased from Merck, India. PABA was purchased from Loba Chemie, India. In the preparation of PABA solution, 1g PABA is dissolved in 15ml of ethanol and made up to 100 ml in a SMF using double distilled Water. Chloride ions concentration of 240 ppm and various concentrations of ferrous ions were prepared using double distilled Water. Corrosion medium is a fixed concentration of 240 ppm of chloride ions in double distilled Water. Inhibitors concentration of 25, 50, 100, 150 and 200 ppm were used to find out corrosion rate and inhibition efficiency.

2.1. Weight loss method

The weight loss measurements were completed according to the standard method as described earlier [18]. In this method, previously polished, degreased and weighed mild steel coupons were immersed in 100mL of 240 ppm chloride ion solution in the absence and presence of various concentrations of inhibitor at ambient temperature. After 24 h immersion, the coupons were taken out from solution, washed with double distilled water, dried carefully and weighed. The weight loss (ΔW) was used to calculate the corrosion rate denoted as CR, (mgdm⁻²day⁻¹) and the inhibition efficiency as IE(%).

$$CR (mg.dm^{-2}.day^{-1}) = W = M_1 - M_2 / SP$$

Where, M_1 and M_2 is the mass of the specimen before and after the corrosion respectively, S is the surface area of the specimen in dm², P is the period of immersion in days, and W is the corrosion rate. The IE was calculated by using the following equation:

$$IE (\%) = (W_0 - W_i) / W_0 \times 100$$

Here $\Delta W = (W_0 - W_i)$, where W_0 and W_i are the corrosion rate of mild steel in the absence and presence of inhibitor respectively,

In this study, the CR value is calculated using the formula,

$$CR (mg.dm^{-2}.day^{-1}) = \Delta W (mg) / [0.096 (dm^2) \times 1 \text{ day}]$$

Where, the surface area S takes the value of 0.096 dm².

2.2. Potentiometric polarization studies

Electrochemical studies were carried out using conventional three electrode cell assembly. The working electrode was a mild steel coupon with a visible surface area of 1 cm² was fixed to a holder and the remaining

area was protected with epoxy coating. Saturated calomel electrode and platinum wire were used as reference and counter electrode. The working electrode was steeply immersed in the test solution and open circuit potential was recorded by using Princeton Applied Research (2 channels) analyzer. With respect to open circuit potential value, the Tafel polarization studies were carried out. Corrosion current (I_{corr}) and corrosion potential (E_{corr}) were obtained by extrapolating the anodic and cathodic curves of Tafel plot. IE was calculated by using corresponding I_{corr} values. Electrochemical impedance analyses were performed in the frequency range from 1 Hz to 1MHz. The mild steel coupons used for this study were 1 cm² surface area which was visible to the corrosive solution. All these measurements were done at atmospheric conditions without any stirring. The experiments were conducted in the absence and presence of inhibitor with different concentration in the 240 ppm chloride ion medium.

2.3. Characterization of surface morphology

The surface morphology of the mild steel coupons in the absence and the presence of optimum concentration of inhibitor were analysed using SEM (TESCAN Vega 3) with electron acceleration between 5 and 10 kV.

2.4. Fourier transforms infrared spectroscopy

FTIR spectra were recorded in Perkin Elmer Spectrum RX I with spectral range of 4000 cm⁻¹ to 400 cm⁻¹ with spectral resolution of 4 cm⁻¹. The mild steel coupons were immersed for 24 h in 100 mL of 240 ppm of aqueous chloride ion medium containing different concentration of PABA. After 24 h, the coupons were taken out and dried. Lastly, the coupons were rubbed with a small amount of KBr powder and made into a disk for FTIR characterization.

2.5. UV-Visible spectroscopy

The UV absorption spectra were recorded for 300 ppm ferrous ion solution, 200 ppm PABA solution and the mixture of ferrous ion and PABA of above concentration using PerkinElmer's Lambda 35 UV-Vis spectrophotometer with spectral range of 190 nm to 1100 nm.

3. Result and Discussion

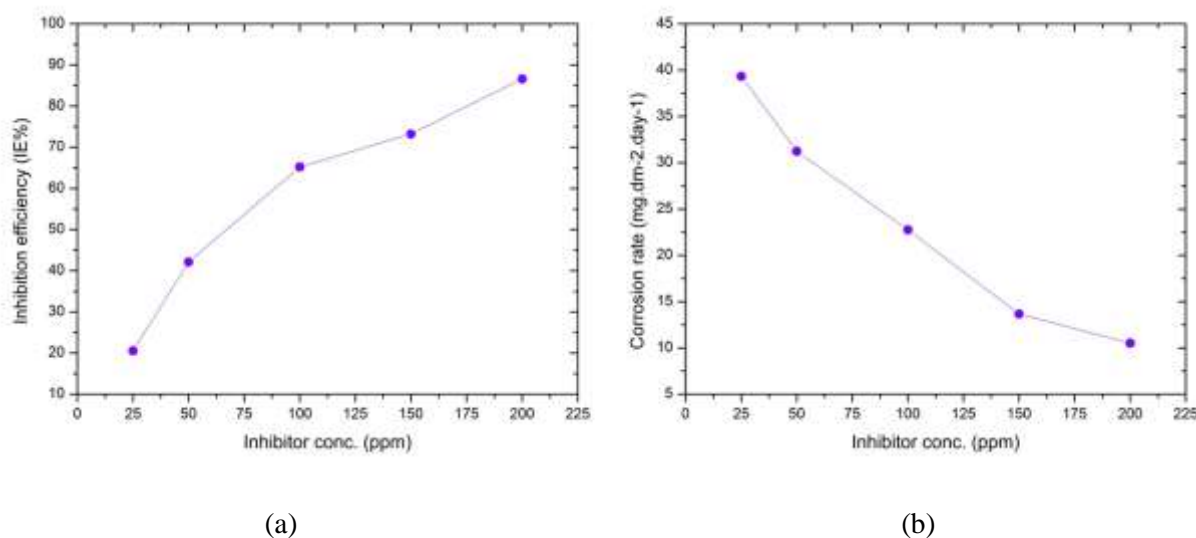
3.1. Weight Loss Measurement

The values of corrosion behaviour of mild steel in 240 ppm chloride ion solution in the absence and presence of various concentration of inhibitor from weight loss measurements are given in Table 1 and figures 2(a) and 2(b). From this study, the IE (%) increases with increase in concentration of the inhibitor. The maximum efficiency 86.61% is obtained at 200 ppm of PABA solution after 24 h of immersion time of mild steel specimens. In figure 2(a), the IE (%) is increasing with inhibitor concentration and the maximum efficiency is reached at a concentration of 200 ppm. On further increasing the inhibitor concentration (250 and 300 ppm) does not show any appreciable change in the efficiency. The reason for this study may be that all the active sites of surface of mild steel are completely adsorbed by the inhibitor molecule and there is no empty active sites available for further adsorption.

Figure 2(b) shows that the CR of mild steel decreases from 31.24 mgdm⁻²day⁻¹ to 5.26 mgdm⁻²day⁻¹ on the addition of 25 ppm to 200 ppm of inhibitor after 24 h of immersion time. The increase in IE (%) from 20.56% to 86.61% may be due to the blocking effect of the metal surface by adsorption and film formation mechanisms, which decreases the effective area of corrosion attack [19]. From the weight loss measurements, the inhibiting performance exhibited by the compound may be due to the presence of donor oxygen atom and π electron of benzene ring, which makes it adsorb and form insoluble protective layer on the surface of mild steel. From these results, it is clear that the studied inhibitor PABA is quickly adsorbed at the corrosion active sites of mild steel surface and responsible for anticorrosion activity.

Table 1. Weight loss studies for mild steel in the absence and presence of various concentrations of inhibitor in 240 ppm chloride ion solution.

Conc. of PABA (ppm)	Weight loss ($mg.dm^{-2}$)	CR ($mg.dm^{-2}.day^{-1}$)	Surface coverage (θ)	IE (%)
Blank	3.93	39.33	-	-
25	3.12	31.24	10.28	20.56
50	2.27	22.76	21.06	42.12
100	1.36	13.67	32.61	65.23
150	1.05	10.53	36.60	73.21
200	0.52	5.26	43.30	86.61

**Figure 2. Weight loss curves of various concentrations of inhibitor in 240 ppm chloride ion solution at room temperature: (a) variation of IE (%) with different concentrations of inhibitor and (b) variation of CR with different concentrations of inhibitor.**

3.2. Potentiodynamic polarization

The PDP curve of mild steel immersed in the absence and presence of inhibitor is shown in figure 3. The corrosion parameters namely E_{corr} , I_{corr} , cathodic slope (β_c), anodic slope (β_a), θ and IE (%) calculated from Tafel plots are given in Table 2.

The IE (%) is defined as

$$IE (\%) = (I_{corr}^0 - I_{corr}) / I_{corr}^0 \times 100$$

Where I_{corr}^0 and I_{corr} is the corrosion current density values without and with inhibitor, respectively.

Electrochemical polarization study of PABA shows that the I_{corr} values decrease with the addition of various concentrations of inhibitor. When the I_{corr} density value decreases, the IE (%) value increases from 12.19 % to 92.06 %. From the observation of the polarization studies, that the I_{corr} values are decreased prominently, the IE (%) increased with increase in the concentration of the inhibitor. The maximum IE (%) obtained at the optimum inhibitor concentration of 200 ppm. Generally, if the value of E_{corr} is greater than 85 mV/SCE the inhibitor can be classified as cathodic or anodic type and however, if the value of E_{corr} is lower than 85 mV/SCE the inhibitor can be classified as mixed-type [20]. The maximum shift E_{corr} values are in the range of 152.88 mV. This shows that the PABA may act as cathodic or anodic type of inhibitor. However, a shift of E_{corr} of the used inhibitor towards anodic side, which is 316.81 to -469.69 mV/SCE, was established (-152.88 mV/SCE). Since the larger displacement exhibited by the used inhibitor is higher than the borderline (-

152.88mV/SCE), it is proved that the addition of inhibitor alters the value of E_{corr} significantly, indicating that the added inhibitor is more polarized in the anodic side. From Table 2, the anodic Tafel plots values were shifted to higher values with reference to blank in the presence of addition of various concentrations of inhibitor when compare to cathodic. These observations confirmed that addition of PABA to 240 ppm chloride ion solution will reduce anodic dissolution of mild steel more than the cathodic hydrogen evolution reaction [21]. All the above fact tells that the used inhibitor is acted as mixed-type corrosion inhibitor, but predominantly anodic.

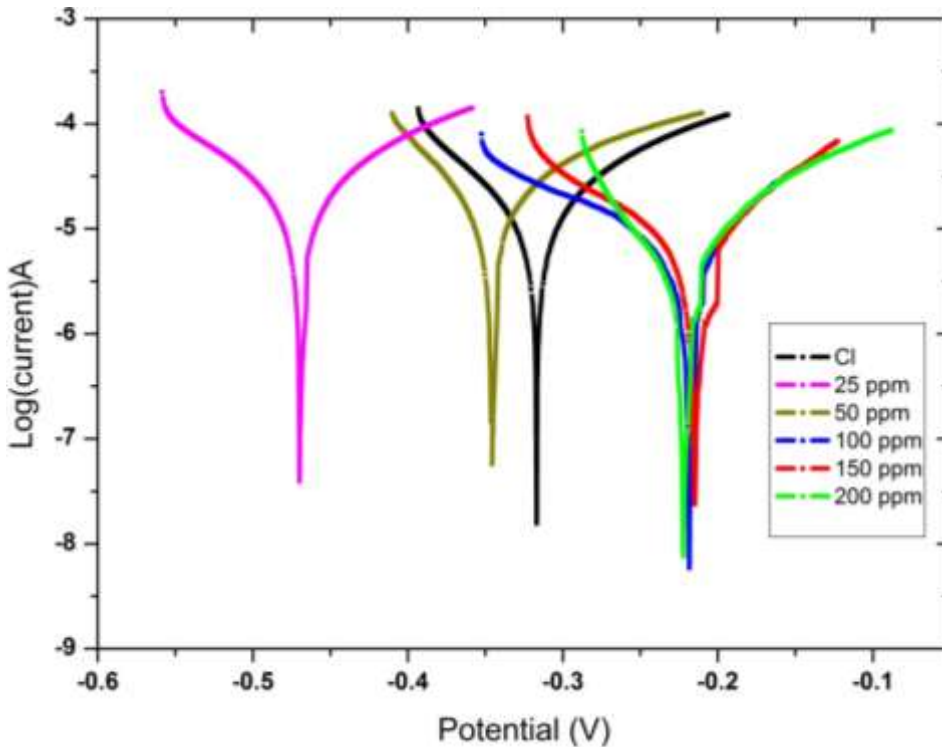


Figure 3. PDP curve for mild steel in 240 ppm aqueous chloride medium in the absence and presence of PABA.

Table 2. PDP parameter for mild steel immersed in 240 ppm aqueous chloride medium in the absence and presence of PABA.

Inhibitor concentration (PPM)	Blank I_{corr} (μAcm^{-2})	Inhibitor I_{corr} (μAcm^{-2})	E_{corr} (mV)/SCE	β_a (mVdec ⁻¹)	β_c (mVdec ⁻¹)	Surface coverage (θ)	IE_{PDP} (%)	IE_{WL} (%)
Blank	23.871	-	-316.81	162.689	128.447	0	-	
25	23.871	20.792	-469.69	121.037	111.39	0.1219	12.19	20.56
50	23.871	18.672	-345.62	86.622	142.007	0.2177	21.77	42.12
100	23.871	4.165	-217.98	118.045	66.397	0.8255	82.55	65.23
150	23.871	4.03	-214.70	87.171	69.131	0.8311	83.11	73.21
200	23.871	1.894	-221.83	45.897	62.891	0.9206	92.06	86.61

3.3. Electrochemical Impedance Spectroscopy

Impedance diagrams obtained for mild steel in 240ppm chloride ion solution in the presence and absence of the inhibitor PABA is shown in figure4. The impedance parameters such as R_{ct} , C_{dl} , Y_{max} , θ and IE (%) is derived from Nyquist plots are given in Table 3.

The equivalent electrical circuit used to fit the impedance spectra for corrosion of mild steel in 240 ppm of aqueous chloride medium in the presence and absence of PABA was shown in Figure 4.

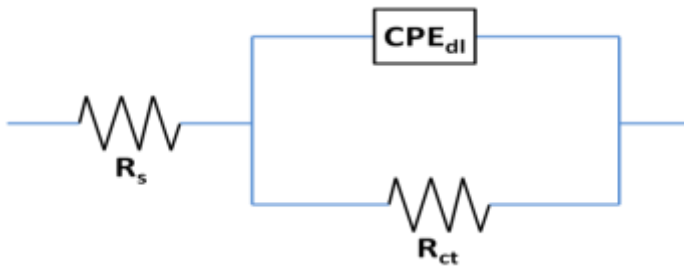


Figure 4. Equivalent electrical circuit used to fit the impedance spectra obtained for mild steel immersed in 240 ppm aqueous chloride medium in the absence and presence of PABA.

The charge transfer resistance increased with an increase in the concentration of inhibitor in 240 ppm chloride ion solution. In the impedance studies,

IE was calculated as: $IE (\%) = (R_{ct(inh)} - R_{ct(b)} / R_{ct(inh)}) \times 100$

Where $R_{ct(b)}$ and $R_{ct(inh)}$ are uninhibited and inhibited charge transfer resistance respectively. The diameter of Nyquist plots increased on increasing the concentration of PABA which indicated the strengthening of inhibitor film [22]. As the concentration of inhibitor increased, charge transfer resistance enhanced and decreased the double layer capacitance values. This was due to the adsorption of PABA on the metal surface leading to the formation of a protective layer on the electrode surface and decreased the extent of dissolution reaction [23-24]. These results were in very good agreement with both weight loss and polarization data and could be attributed to decreased local dielectric constant and increased thickness of the electrical double layer [25].

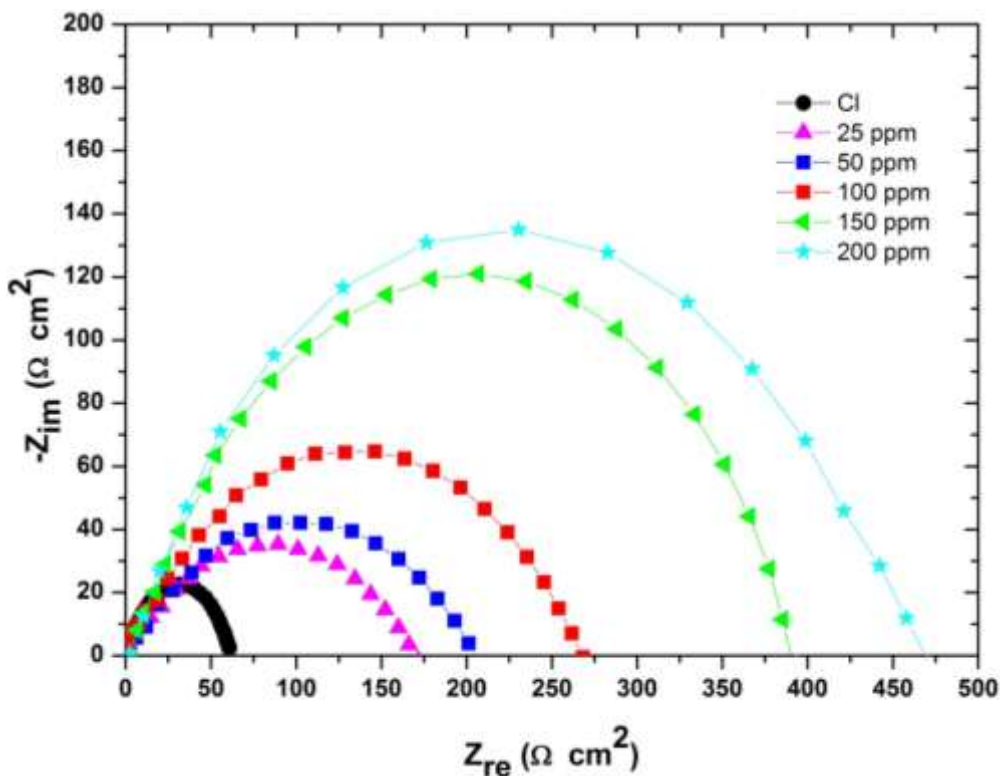


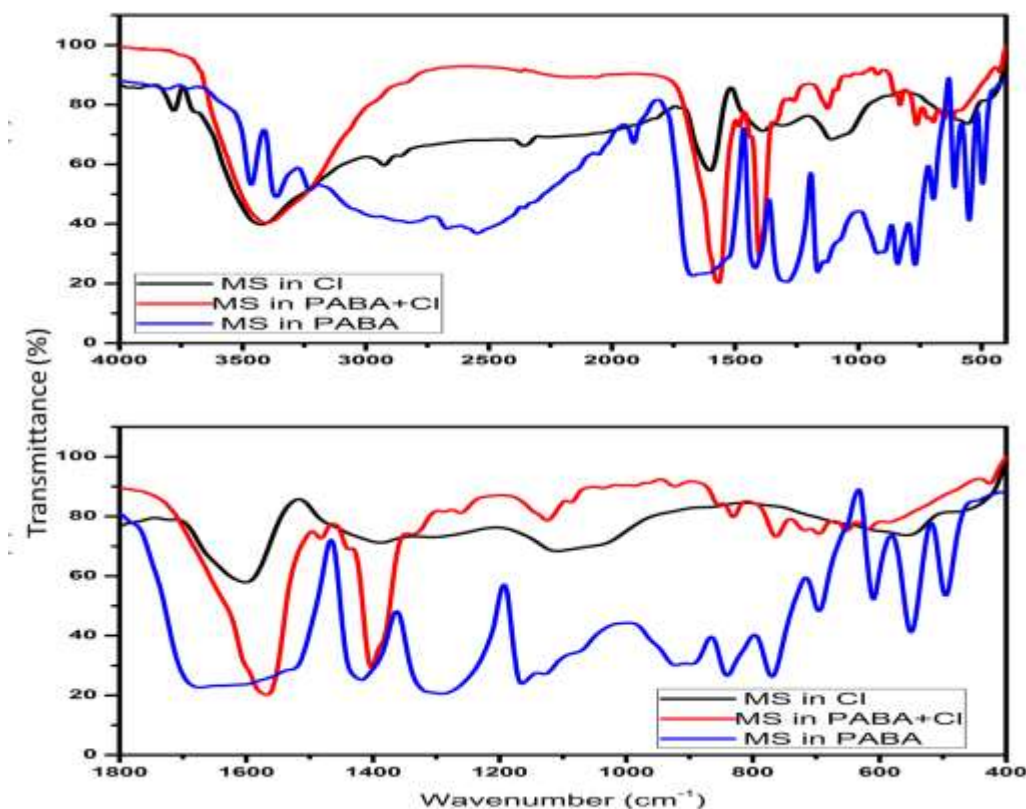
Figure 5. Electrochemical impedance (Nyquist) spectrum of mild steel in 240 ppm chloride ion solution with and without various concentrations of inhibitor.

Table 3. Linear polarization resistance parameters values for corrosion of mild steel in 240 ppm chloride ion solution containing various concentrations of inhibitor.

Inhibitor	PABA concentration (ppm)	R_{ct} ($\Omega \text{ cm}^2$)	C_{dl} ($\mu \text{ F cm}^{-2}$)	IE (%)
PABA	0 (Blank)	62.32	-	-
	25	174.91	1.04	64.37
	50	239.35	5.56	73.96
	100	352.59	2.56	82.32
	150	436.7	1.67	85.73
	200	529.18	1.13	88.22

3.4 Analysis of adsorbed film

The scraped mild steel samples collected from specimen immersed in 240 ppm aqueous chloride medium is labeled as "MS in Cl" and scraped samples collected from specimen immersed in the same chloride medium with PABA are labeled as "MS in PABA+Cl" and were used in the below discussion. The FTIR spectra in Figure 6 were recorded for MS in Cl, MS in PABA+Cl and MS in PABA samples.

**Figure 6. FTIR spectra of mild steel in chloride medium, in PABA and chloride medium and in PABA**

The FTIR spectra in Figure 6 were recorded for MS in Cl, MS in PABA+Cl and PABA samples. The strong peaks at 3466, 3363 and 3227 cm^{-1} corresponds to $-\text{NH}$ stretching of the amine group. The strong peaks at 1661 cm^{-1} was due to the carbonyl group of PABA. The shift in the carbonyl peak indicates the interaction of carbonyl group of PABA with the surface of the mild steel. The peaks at 1600, 1573 and 1524 cm^{-1} corresponds to the $\text{C}=\text{C}$ vibrations of the PABA[26]. These peaks shifted after adsorption of PABA, which implies there is an interaction between the aromatic ring and the mild steel. The disappearance of the strong peak at 1310 cm^{-1} clearly indicated that there is an interaction with nitrogen of $\text{C}-\text{N}$ bond with the metal surface.

The UV-Vis absorption spectrum in Figure 7 was taken for 200 ppm of PABA, optimum concentration of Fe (FeSO_4), and 200 ppm PABA& optimum concentration of Fe. The formation of new bands and shift in the absorption band clearly show that there is effective complex formation between Fe^{2+} ion and PABA.

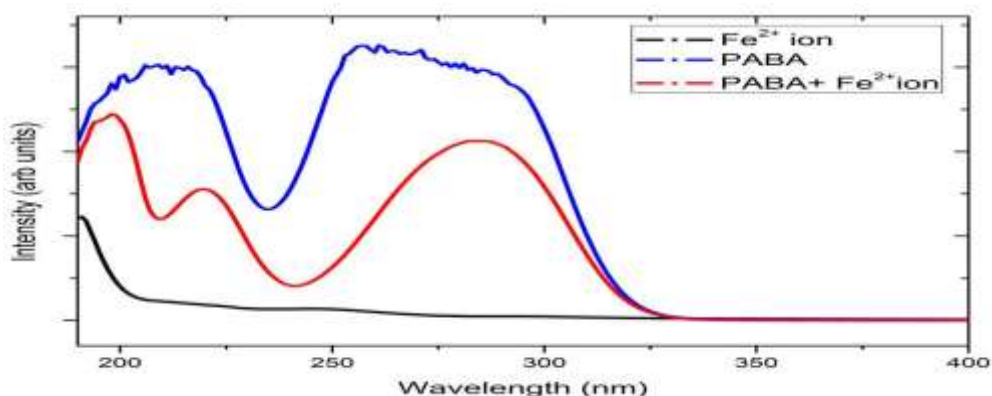


Figure 7. UV-Vis spectrum for pure Fe^{2+} , PABA, and Fe^{2+} +PABA

3.5. Surface analysis

The surfaces of mild steel were analysed using SEM after 24h immersion in 240 ppm chloride ion solution in the absence and presence of optimum (200 ppm) concentration of inhibitor. The SEM images of polished mild steel, 240 ppm chloride ion solution without inhibitor, and 240 ppm chloride ion solution with inhibitor are given in Figures 8(a)–8(c). The Figure 8(c) indicates that the anticorrosion activity is increased remarkably in the presence of inhibitor due to the effective adsorption of PABA.

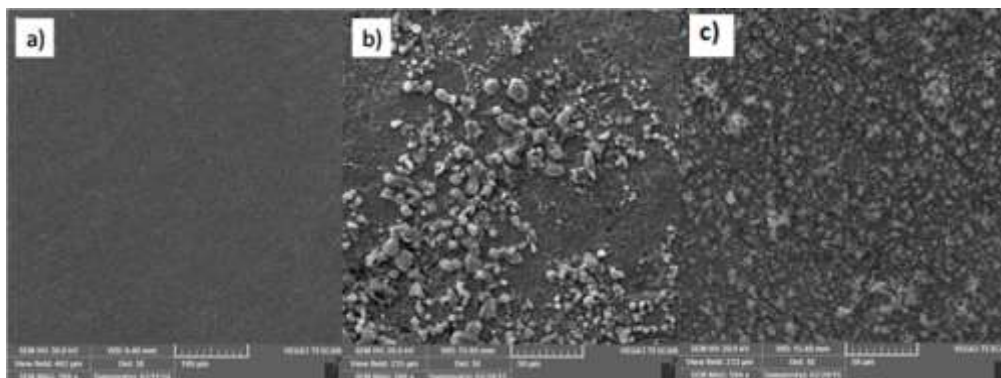


Figure 8. SEM images of the surface of mild steel: (a) polished mild steel, (b) after immersion in 240 ppm chloride ion solution in absence of PABA and (c) in presence of PABA.

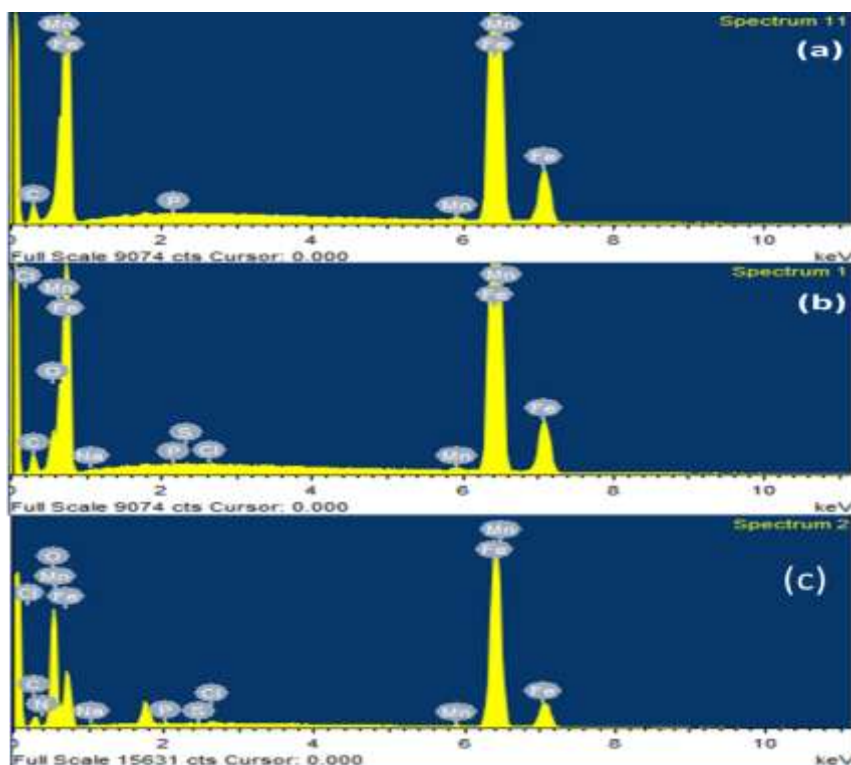


Figure 9.EDS spectra of the surface of mild steel: a) polished mild steel b) mild steel immersed in 240 ppm of aqueous chloride medium and c) mild steel immersed in 240 ppm of aqueous chloride medium in presence of VB10.

The corresponding EDS spectra to the SEM image Figures 8(a) to 8(c) were shown in Figures 9(a) to 9(c). In Figure 9(b), the presence of chloride ion was responsible for the pitting in the mild steel seen in Figure 8(b). Sodium ions were confirmed to have no influence on the corrosion behavior.[41]The presence of nitrogen atom in Figure 9(c) implied that the inhibitor VB10 was adsorbed on the mild steel and smooth SEM images of VB10 seen in Figure 8(c).

4. Conclusion

1. PABA is found to be worthy green inhibitor for mild steel in 240 ppm chloride ion solution.
2. Corrosion inhibition property was increased with increase in inhibitor concentration.
3. EIS study shown that the studied inhibitor follows adsorption mechanism and controls the corrosion of mild steel in 240 ppm chloride ion solution.
4. Polarization studies show that PABA acts as a mixed-type corrosion inhibitor, but predominantly anodic inhibitor.
5. IE (%) obtained from weight loss measurement was in good agreement with EIS and PDP methods.
6. FTIR and UV study show that there is a complex formation between Fe and PABA.
7. SEM & EDS studies confirmed the formation of inhibitor film on the surface of mild steel.

5. Reference

1. Amin, M. A.; Khaled, K. F.; Mohsen, Q.; Arida, H. A. A study of the inhibition of iron corrosion in HCl solutions by some amino acids. *Corros.Sci.* 2010, 52, 1684.
2. Veawab, A.; Tontiwachwuthikul, P.; Chakma, A. Corrosion behaviour of carbon steel in the CO₂ absorption process using aqueous amine solutions. *Ind. Eng. Chem. Res.* 1999, 38, 3917.
3. Touhami, F.; Aouniti, A.; Abed, A.; Hammouti, B.; Kertit, S.; Ramdani, A.; Elkacemi, K. Corrosion inhibition of armco iron in 1 M HCl media by new bipyrazolic derivatives. *Corros.Sci.* 2000, 42, 929.
4. Darwish, N. A.; Hilbert, F.; Lorenz, W. J.; Rosswag, H. The influence of chloride ions on the kinetics of iron dissolution. *Electrochim.Acta* 1973, 18, 421.

5. Yao, J. L.; Ren, B.; Huang, Z. F.; Cao, P. G.; Gu, R. A.; Tian, Z.-Q. Extending surface Raman spectroscopy to transition metals for practical applications IV.A study on corrosion inhibition of benzotriazole on bare Fe electrodes. *Electrochim. Acta* 2003, 48, 1263.
6. Veawab, A.; Tontiwachwuthikul, P.; Bhole, S. D. Studies of corrosion and corrosion control in a CO₂-2-amino-2-methyl-1-propanol (AMP) environment. *Ind. Eng. Chem. Res.* 1997, 36, 264.
7. Lai, B.; Zhou, Y.; Yang, P. Passivation of sponge iron and GAC in Fe₀/GAC mixed-potential corrosion reactor. *Ind. Eng. Chem. Res.* 2012, 51, 7777.
8. Veawab, A.; Tontiwachwuthikul, P.; Chakma, A. Investigation of low-toxic organic corrosion inhibitors for CO₂ separation process using aqueous MEA solvent. *Ind. Eng. Chem. Res.* 2001, 40, 4771.
9. Zerfaoui, M.; Oudda, H.; Hammouti, B.; Kertit, S.; Benkaddour, M. Inhibition of corrosion of iron in citric acid media by amino acids. *Prog. Org. Coat.* 2004, 51, 134.
10. Abdel-Rehim, S. S.; Khaled, K. F.; Al-Mobarak, N. A. Corrosion inhibition of iron in hydrochloric acid using pyrazole. *Arabian J. Chem.* 2011, 4, 333.
11. Feng, Y.; Chen, S.; Guo, W.; Zhang, Y.; Liu, G. Inhibition of iron corrosion by 5,10,15,20-tetraphenylporphyrin and 5,10,15,20-tetra-(4-chlorophenyl)porphyrin layers in 0.5 M H₂SO₄ solutions. *J. Electroanal. Chem.* 2007, 602, 115.
12. Zhang, Z.; Chen, S.; Li, Y.; Li, S.; Wang, L. A study of the inhibition of iron corrosion by imidazole and its derivatives self assembled films. *Corros. Sci.* 2009, 51, 291.
13. Sagues, A. A.; Davis, B. H.; Johnson, T. Coal liquids distillation tower corrosion. Synergistic effects of chlorides, phenols, and basic nitrogen compounds. *Ind. Eng. Chem. Process Des. Dev.* 1983, 22, 15.
14. Wahbi, Z.; Guenbour, A.; Abou El Makarim, H.; Ben Bachir, A.; El Hajjaji, S. Study of the inhibition of the corrosion of iron steel in neutral solution by electrochemical techniques and theoretical calculations. *Prog. Org. Coat.* 2007, 60, 224.
15. Colorado-Garrido, D.; Ortega-Toledo, D. M.; Hernández, J. A.; González-Rodríguez, J. G.; Uruchurtu, J. Neural networks for Nyquist plots prediction during corrosion inhibition of a pipeline steel. *J. Solid State Electrochem.* 2009, 13, 1715.
16. Tao, Z.; Zhang, S.; Li, W.; Hou, B. Adsorption and corrosion inhibition behaviour of mild steel by one derivative of benzoic-triazole in acidic solution. *Ind. Eng. Chem. Res.* 2010, 49, 2593.
17. Lukovits, I.; Kalman, E.; Zucchi, F. Corrosion inhibitors correlation between electronic structure and efficiency. *Corrosion* 2001, 57, 3.
18. Ganapathi Sundaram, R.; Karthik, G.; Vengatesh, G.; Sundaravadivelu, M. Adsorption characteristics of Kynurenic acid as green corrosion inhibitor at mild steel / hydrochloric acid interface. *Der Chemica Sinica* 2015, 6, 54.
19. Zhao, T.; Mu, G. The adsorption and corrosion inhibition of anion surfactants on aluminium surface in hydrochloric acid. *Corrosion Science* 1999, 41, 1937.
20. Verma, C.B.; Quraishi, M.A. Schiff's bases of glutamic acid and aldehydes as green corrosion inhibitor for mild steel: weight loss, electrochemical and surface analysis. *International journal of innovative research in science, engineering and technology* 2014, 3, 14601.
21. Musa, A.Y.; Mohamed, A.B.; Takriff, M.S.; Jalgham, R.T.T. Electrochemical and quantum chemical studies on phthalhydrazide as corrosion inhibitor for mild steel in 1 M HCl solution. *Research on Chemical Intermediates* 2012, 38, 453.
22. Taleb, I.; Mehad, H.; Corrosion inhibition of mild steel in 2M HCl using aqueous extract of eggplant peel. *Int. J. Electrochem. Sci.* 2011, 6, 5357.
23. Vinodkumar, K.P.; Narayanan Pillai, M.S.; Rexin Thusnavis, G. Pericarp of the Fruit of *Garcinia Mangostana* as Corrosion Inhibitor for Mild Steel in Hydrochloric Acid Medium. *P Electrochim. Acta* 2010, 28, 373.
24. Sobhi, M.; Abdallah, M.; Khairou, K.S. Sildenafil Citrate (viagra) as corrosion inhibitors for carbon steel in hydrochloric acid solutions. *Monatsh. Chem* 2012, 143, 1379.
25. Ibrahim, T.; Habbab, M. Corrosion inhibition of mild steel in 2M HCl using aqueous extract of Eggplant peel. *Int. J. Electrochem. Sci.* 2011, 6, 5357.
26. Roik, N.V.; Belyakova, L.A. IR Spectroscopy, X-Ray Diffraction and Thermal Analysis Studies of Solid "β-Cyclodextrin - Para-Aminobenzoic Acid " Inclusion Complex. *PHYSICS AND CHEMISTRY OF SOLID STATE*, 2011, 12, 168.
